

Photo-induced electron transfer between hypocrellins and nano-sized semiconductor CdS

—EPR study on the kinetics of photosensitized reduction in HA-CdS and HB-CdS systems

ZHOU Zhixiang (周志祥), LIU Wei (刘 卫), WANG Fuyuan (王芙媛)
& ZHANG Zhiyi (张志义)

Institute of Biophysics, Chinese Academy of Sciences, Beijing 100101, China

Correspondence should be addressed to Zhang Zhiyi (email: zhangzhy@sun5.ibp.ac.cn)

Received September 25, 2000

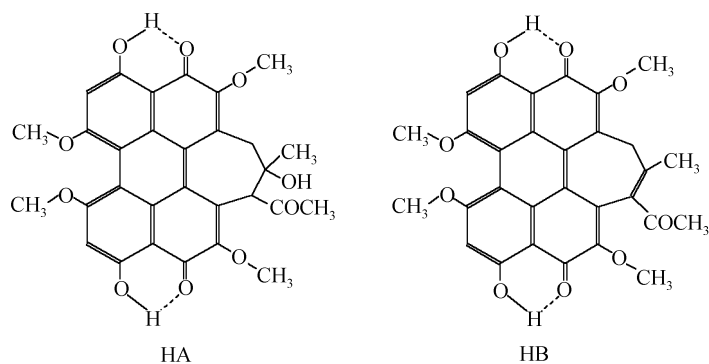
Abstract Both HA-CdS and HB-CdS (Hys-CdS, Hys represents HA, HB) complex systems were established according to the dynamics of heterogeneous electron-transfer process $\mu = E_{S^*/S^+} - E_{CB} < 0$. In these systems, the electron transferring from $^1\text{Hys}^*$ to conduction band of CdS is feasible. Determined from the fluorescence quenching, the apparent association constants (K_{app}) between Hypocrellin A (HA), Hypocrellin B (HB) and CdS sol. were about $940 (\text{mol/L})^{-1}$, $934 (\text{mol/L})^{-1}$, respectively. Fluorescence lifetime measurements gave the rate constant for the electron transfer process from $^1\text{HA}^*$, $^1\text{HB}^*$ into conduction band of CdS semiconductor as $5.16 \times 10^9 \text{ s}^{-1}$, $5.10 \times 10^9 \text{ s}^{-1}$, respectively. TEMPO (2,2,6,6-tetramethyl-1-piperidinyloxy), a stable nitroxide radical, was used in the kinetic study of the reduction reaction taking place on the surface of a CdS colloidal semiconductor, kinetics equation of the reaction was determined with the electron paramagnetic resonance (EPR) method, and the reaction order of TEMPO is zero. When Hys were added, the rate of EPR increased greatly. By comparing rate constants, the Hys-CdS systems were revealed to be about 350 times more efficient than CdS sol. alone in the photoreduction of TEMPO under visible light. It suggests that Hys can be used as efficient sensitizers of a colloidal semiconductor in the application of solar energy.

Keywords: photosensitizer HA, HB (Hys), nano-sized semiconductor CdS, apparent association constant (K_{app}), TEMPO, rate constant, EPR.

Nano-sized semiconductors fall into the transition state between molecular and bulk material properties. Such ultrasmall particles possess unique catalytic behavior and show size quantization effects, nonlinear optical properties^[1], and have been widely applied as light energy conversion materials^[2]. But one disadvantage for large band-gap semiconductor is that its photoactivity is limited to the UV region. In addition, the separated electron can easily recombine with hole to release heat or light before reaching the surface.

Hence, photosensitization of semiconductor particle by visible light absorbent has been widely used as a means to shift the semiconductor catalytic activity to longer wavelength^[3]. That is, in visible light, photosensitizer acting as an "antenna molecule" can be excited to its excited

state, and the electron will be injected into the conduction band of semiconductor from the excited photosensitizer. As a result, the spectral response is extended to visible light range, and the photo-generated electron-hole pairs are separated efficiently. Therefore, the study of the electron-transferring process between photosensitizer and semiconductor and the kinetics of photosensitized reduction taking place on the surface of the semiconductor are very useful in solar energy exploitation^[4].



Two kinds of peryloquinone derivative, Hypocrellin A and Hypocrellin B (Hys), have been proved to have unique photosensitization properties^[5], and nano-sized semiconductor CdS is one important light-energy conversion material^[6]. The oxidation potential of ${}^1\text{HA}^*$, $E_{1\text{HA}^*} = -1.56$ V (vs. NHE), $E_{1\text{HB}^*} = -1.55$ V (vs. NHE); the energy level of the conduction band of CdS, which lies around -1.00 V (vs. NHE)^[7], thus according to the dynamics of heterogeneous electron-transfer process $\mu = E_{S^*/S^+} - E_{\text{CB}} < 0$, there is favorable energy for such a charge injection process from ${}^1\text{Hys}^*$ to CdS.

Techniques, such as laser flash photolysis, resonance Raman spectroscopy, diffuse reflectance and so on, have been used to investigate the charge injection process between photosensitizer and semiconductor^[8,9]. But the kinetics and the nature of photoreduction reaction taking place on their surfaces have not been well understood. Such information is of course important in the design of more efficient photoelectrochemical reaction system. EPR is a favorable method in the study of kinetics because the EPR can measure the concentration change of spin material at any time without interfering with the action. So when an appropriate spin material is selected, the photoelectrochemical reaction of colloidal semiconductor can be investigated conveniently. Methyl violet (MV^{2+}) has been used as an electron acceptor to investigate the photo-induced electron reaction, $e^- + \text{MV}^{2+} \rightarrow \text{MV}^{\cdot+}$ ^[10]. But MV^{2+} is not a good electron acceptor because of its dimeric reaction, especially, the reaction $e^- + \text{MV}^{2+} \rightarrow \text{MV}^{\cdot+}$ will be held back even though only a minim O_2 exists in the system.

TEMPO (2,2,6,6-tetramethyl-1-piperdinyloxy) is a free radical. After it accepts an electron and a proton, its EPR signal will be lost. In this article, taking TEMPO as an electron acceptor and

using EPR method, a process of photoreduction reaction which took place on the surface of CdS semiconductor was investigated and the kinetic equation of the reaction was established. By comparing rate constants, the Hys-CdS systems were revealed to be about 350 times more efficient than CdS sol. alone in the photoreduction of TEMPO under visible light. It is proved that Hys can improve photochemical efficiency of CdS sol. in visible light intensively.

1 Experimental

1.1 Materials

CdCl₂, Na₂S and hexametaphosphate (HMP) were of analytical grades. 2,2,6,6-tetramethyl-1-piperdinyloxy (TEMPO) was obtained from Aldrich Chemical Company. Triton X-100 was purchased from FARCO Chemical Company. They were all used without further purification. Redistilled water was used in all experiments.

HA and HB were obtained from the Microbiology Institute of Yunnan Province, People's Republic of China. It was recrystallized twice in acetone and dispersed in water using Triton X-100 with occupancy number 1 : 1^[11].

1.2 Preparation of CdS colloidal semiconductor

At 0°C, CdCl₂ solution was added rapidly under vigorous stirring to the solution containing equal mol Na₂S and HMP (HMP is the stabilizer of sol.). The average diameter obtained from JEM-100CX transmission electron microscopy is about 15 nm.

1.3 Measurements of the oxidation potential of HA, HB

Fig. 1 is the cyclic voltammograms of HB. The curve was obtained from Electro-Chemical system (PAR370, EG&G, American) at 22°C ± 1°C in 0.1 mol/L KCl solution (pH ≈ 7.0); working electrode: Pt-electrode; reference and assistant electrode: saturated calomel electrode and Pt, respectively. According to fig. 1, the oxidation potential of ⁰HB (E_{HB}) was 0.52 V (vs. NHE). In the same way, the oxidation potential of ⁰HA (E_{HA}) was 0.54 V (vs. NHE). The excited energies of singlet state (E_{s1}) of HA, HB were 2.10 eV, and 2.07 eV, respectively^[12], and $E_{1Hys^*} = E_{Hys/Hys^*} - E_{s1}$, so E_{1HA^*} and E_{1HB^*} were -1.56 V (vs. NHE), -1.55 V (vs. NHE), respectively.

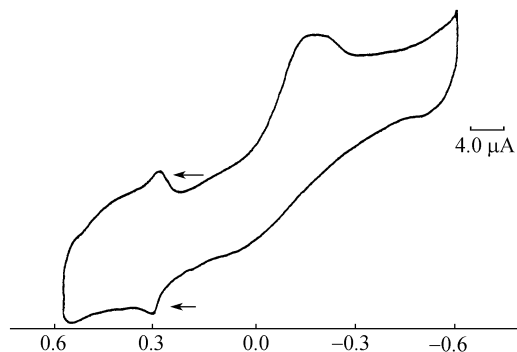


Fig. 1. The cyclic voltammogram of HB in Triton X-100 solution (occupancy number 1 : 1). $V = 50$ mV/s, $[HB] = 5.00 \times 10^{-5}$ mol/L, pH = 7.0.

1.4 Hys-CdS complex system and absorption spectra character

Both HA-CdS and HB-CdS complex systems were established according to the dynamics of heterogeneous electron-transfer process $\mu = E_{S^*/S^+} - E_{CB} < 0$. In these systems, the electron

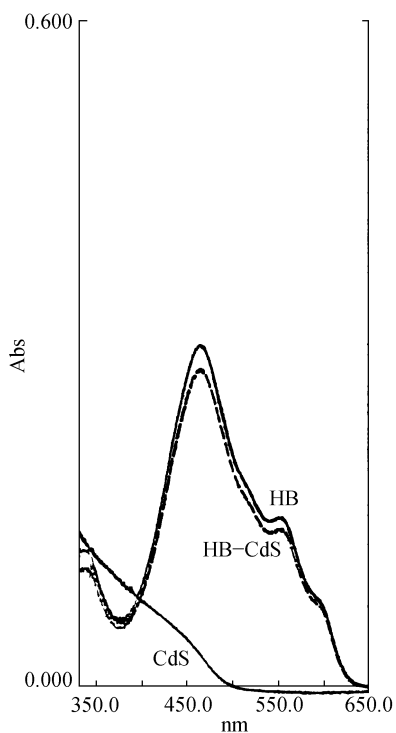


Fig. 2. Absorption spectra of CdS sol., HB and HB-CdS system. $[CdS] = 6.00 \times 10^{-5}$ mol/L, $[HB] = 1.67 \times 10^{-5}$ mol/L.

transferring from $^1Hys^*$ to conduction band of CdS is feasible. Absorption spectra were recorded with a Hitachi U-3200 spectrophotometer. The absorption spectra of HB in Triton X-100 solution with occupancy number 1 : 1, recorded in the presence and in the absence of CdS semiconductor sol., are shown in fig. 2. The percentage absorbance of HB is characterized by the intense band located at 470 nm assigned to the molecular band. In the presence of colloidal CdS this peak decreased markedly, but the location of the peak did not change. It is due to adsorption partly on the surface of CdS semiconductor.

1.5 Apparent association constant (K_{app}) measurements

Emission spectra were recorded with a Hitachi-F4500 fluorescence photometer at $22^\circ C \pm 1^\circ C$.

1.6 Fluorescence lifetime measurements

The picosecond laser system utilized a Spectra Physics M3800 CW Nd : YAG Laser with a Spectra Physics M3500 Ultrashort Pulse Dye Laser (rhodamine 6G) and Spectra Physics M3295 Cavity Dumper operated at 800 kHz. The dye laser was operated at 580 nm. The fluorescence lifetime measurements were carried out on a time-correlated single-photon-counting spectrofluorometer system (EG&G). The photons were detected by a Hamamatsu E3059-00 microchannel plate photomultiplier.

1.7 Irradiation light source

A 1000 W Halogen-W lamp was used as light source in the visible range. The light passed through a filter with cooling water to remove UV and infrared irradiation, then through a lens and focused on the sample in a quartz capillary with an irradiation intensity of $400 W/m^2$ measured by a BTY-820 radiometer. The irradiation time was controlled by a special accessory.

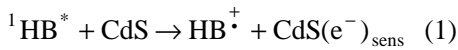
1.8 EPR measurement of spin counteraction

Samples were injected into quartz capillaries for EPR analysis. The EPR spectra were obtained at room temperature ($20^\circ C \pm 2^\circ C$), X-band. Unless otherwise stated, the EPR parameters were: microwave power 10 mW, amplitude modulation 1.0×10^{-4} T, time constant 0.128 s, scan rate 4 min. Samples were continuously irradiated. The height of the middle peak of the EPR first-derivative spectra is in direct proportion to the concentration of TEMPO. 1 mol/L NaOH and 1 mol/L HCl were used to modulate the pH scale of the solution.

2 Results and discussion

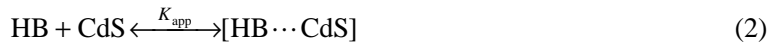
2.1 Apparent association constant K_{app}

Addition of CdS sol. to a solution of HB resulted in the quenching of its fluorescence emission (fig. 3). This quenching behavior is similar to the previously reported fluorescence quenching of dyes like Anthracene-9-carboxylic^[3], Chlorophyllin^[8] and is attributed to the charge injection from the excited singlet of HB to the conduction band of CdS (reaction 1).



The oxidation potential of ${}^1\text{HB}^*$, which is -1.55 V (vs. NHE), and the energy level of the conduction band of CdS, which lies around -1.00 V (vs. NHE, pH 7.0)^[7], provide favorable energy for such a charge injection process.

Based on the fluorescence quenching behavior, the participation of CdS in the quenching process was further analyzed by considering the equilibrium between adsorbed and unadsorbed molecules of the sensitizers with an apparent association constant K_{app} (reaction 2).



The observed quantum $\phi_{f(\text{obsd})}$ of HB in a colloidal CdS suspension can be related to the fluorescence yields of unadsorbed (ϕ_f^0) and adsorbed (ϕ_f') molecules of HB by the equation:

$$\phi_{f(\text{obsd})} = (1 - \alpha)\phi_f^0 + \alpha\phi_f', \quad (3)$$

where α is the degree of association between HB and CdS. At relatively high CdS concentration,

$$\alpha = (K_{app}[\text{CdS}]) / (1 + K_{app}[\text{CdS}]) \quad (4)$$

then eq. (3) could then be simplified to

$$(\phi_f^0 - \phi_{f(\text{obsd})})^{-1} = (\phi_f^0 - \phi_f')^{-1} + \{K_{app}(\phi_f^0 - \phi_f')\}[\text{CdS}]^{-1}. \quad (5)$$

If the quenching is due to the association of HB with CdS, one would expect a linear dependence of $(\phi_f^0 - \phi_{f(\text{obsd})})^{-1}$ on the reciprocal concentration of CdS sol. with an intercept equal to $(\phi_f^0 - \phi_f')^{-1}$ and a slope equal to $(K_{app}(\phi_f^0 - \phi_f'))^{-1}$. The straight plot observed in the insert of fig. 3 confirms the assumption above. By eq. (5), the value of K_{app} determined from this plot was 934 (mol/L)⁻¹. In the same way, the apparent association constant of HA-CdS was 940

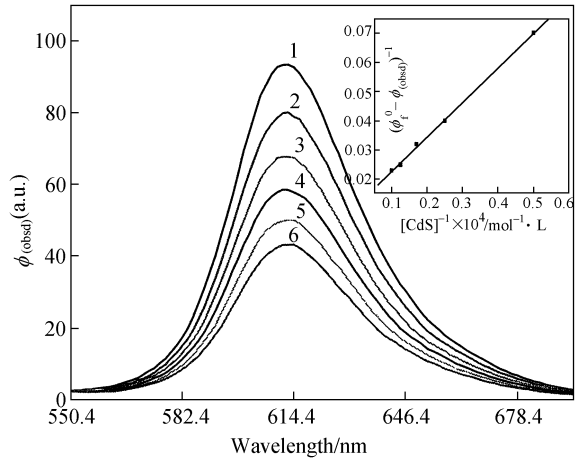


Fig. 3. Fluorescence emission spectra of 2.20×10^{-5} mol/L HB in aqueous solution at various concentrations of CdS: 1, 0 mol/L, 2, 2.00×10^{-4} mol/L, 3, 4.00×10^{-4} mol/L, 4, 6.00×10^{-4} mol/L, 5, 8.00×10^{-4} mol/L, 6, 1.00×10^{-3} mol/L. The excitation wavelength was at 466 nm. The inset shows the dependence of $(\phi_f^0 - \phi_{f(\text{obsd})})^{-1}$ on $[\text{CdS}]^{-1}$.

(mol/L)⁻¹. This suggests that there are complexes associated between Hys and CdS semiconductor, which is an essential requisite for observing the heterogeneous charge-transfer process at the interface of sensitizer-semiconductor.

2.2 Fluorescence lifetime measurements

In order to further analyze the fluorescence quenching process, fluorescence lifetime measurements were performed. It has been shown that the sensitizer molecules adsorbed on the TiO₂ surface had a significantly shorter excited singlet lifetime than in homogeneous solution and this decrease in lifetime could be correlated with the charge injection process^[3]. For example, in the absence of CdS, the fluorescence lifetime of HA exhibits a single-exponential decay ($F(t) = A \times \exp(-t/\tau)$) with a lifetime of 1.07 ns. However, in a CdS suspension, the fluorescence emission of HA followed a two-exponential decay ($F(t) = A_1 \exp(-t/\tau_1) + A_2 \exp(-t/\tau_2)$). The fluorescence decay for HA in 5.00×10^{-5} mol/L CdS suspension is shown in fig. 4 (curve 1). There is an obvious component with a much shorter lifetime. A component with a lifetime similar to that of HA alone was also observed. Computer analysis of the decay gives a lifetime of 0.159 ns for the shorter lived component, which is assumed to be due to the adsorbed dye. The lifetime of the longer lived component is 0.886 ns, which is close to the lifetime of HA in CdS free solution (1.07 ns).

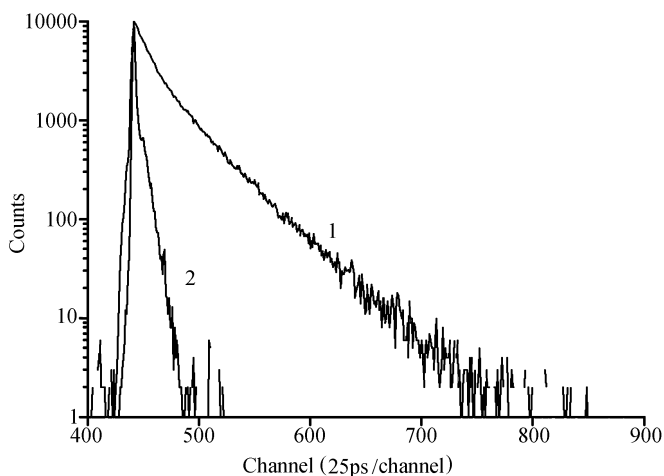


Fig. 4. Fluorescence decay and normalized instrument response curves for a sample of 2.00×10^{-5} mol/L HA in 5.20×10^{-5} mol/L CdS. Excitation was 580 nm, emission was recorded at 600 nm, $A_1 = 0.124$, $\tau_1 = 0.886$ s, $A_2 = 0.359$, $\tau_2 = 0.159$ s, $\chi^2 = 1.313$.

If we suppose that the observed decrease in fluorescence lifetime is entirely due to the electron injection process and the other radiation and nonradiation decay processes of HA associated with CdS colloid occur at the same rates as in neat solvent, we can correlate the observed lifetimes by the following expression^[3]:

$$1/\tau_{\text{ads}} = 1/\tau + K_{\text{et}}, \quad (6)$$

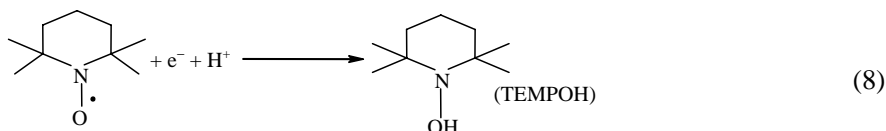
where τ and τ_{ads} are the lifetimes of the sensitizer in aqueous solution and adsorbed on to the CdS surface, and K_{et} is the specific rate of the charge injection process from excited singlet state of HA to conduction band of CdS semiconductor. The value of K_{et} obtained upon substitution of the values of τ and τ_{ads} in eq. (6) was $5.16 \times 10^9 \text{ s}^{-1}$. And for HB-CdS system, the value of K_{et} is $5.10 \times 10^9 \text{ s}^{-1}$.

2.3 The kinetics equation of photoreduction

Electron-hole pair was generated when CdS semiconductor was irradiated by light.



TEMPO can be degraded after accepting an electron and a proton (reaction 8),



The reduced production (TEMPOH) of TEMPO cannot be detected in EPR because it does not have an unpaired electron. And the concentration of TEMPO is in direct proportion to the height of the middle peak. So after TEMPO accepted the e_{CB}^- (reaction (8)), the height of its EPR spectra would decrease.

The initial rate of reaction (8) can be expressed as

$$V_0 = -d[\text{TEMPO}]/dt = k'[\text{H}^+]^a [e_{\text{CB}}^-]^m [\text{TEMPO}]^n, \quad (9)$$

where k' is the rate constant, a , m and n are reaction orders of H^+ , e_{CB}^- and TEMPO, respectively. In this experiment, the scale of pH was kept constant in buffer solution, so $k = k'[\text{H}^+]^a$. And e is only from CdS, so $e_{\text{CB}}^- \propto [\text{CdS}]$. Eq. (9) will then be simplified to

$$V_0 = -d[\text{TEMPO}]/dt = k[\text{CdS}]^m [\text{TEMPO}]^n. \quad (10)$$

According to eq. (10), when keeping $[\text{CdS}]$ (or TEMPO) constant, one would expect a linear dependence of $\lg(V_0)$ on $\lg[\text{TEMPO}]$ (or $\lg[\text{CdS}]$), and the slope is n (or m). This was confirmed by the plots in fig. 5 (line 1) and fig. 6. We can determine $n = 0.01 \approx 0$, $m = 0.95 \approx 1$. Besides this, one should expect a linear dependence of $\lg t_{1/2}$ on $\lg[\text{TEMPO}]$. This is confirmed by plot 1 in fig. 7, and the slope is $1-n$. The plot's slope is 0.93, so $n = 0.07 \approx 0$.

The change in trend of C/C_0 depending on $\lg(t)$ of some common reaction orders was plotted^[13] as a Powell plot in fig. 8(a). In a plot of C/C_0 vs. $\lg t$, any reaction of the same order is of the same figure but different A value. A plot of $[\text{TEMPO}]/[\text{TEMPO}]_0$ vs. $\lg t$ was made (fig. 8(b)). The plot 1 of fig. 8(b) fits curve 1 on the Powell plot perfectly. This means that the reaction order of TEMPO is zero.

So, eq. (10) can be simplified to

$$V_0 = -d[\text{TEMPO}]/dt = k[\text{CdS}]. \quad (11)$$

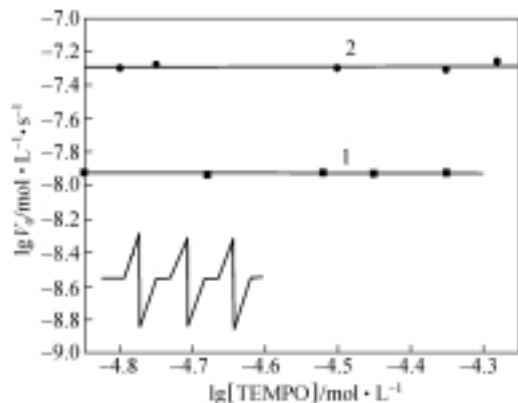


Fig. 5. Initial rate (V_0) of degradation of TEMPO vs. the concentration of TEMPO. 1, $[\text{CdS}] = 6.00 \times 10^{-5} \text{ mol/L}$; 2, $[\text{CdS}] = 6.00 \times 10^{-5} \text{ mol/L}$, $[\text{HB}] = 1.00 \times 10^{-5} \text{ mol/L}$. Inset: a typical EPR spectrum of TEMPO ($a_N = 16.3 \times 10^{-4} \text{ T}$; $g = 2.0056$).

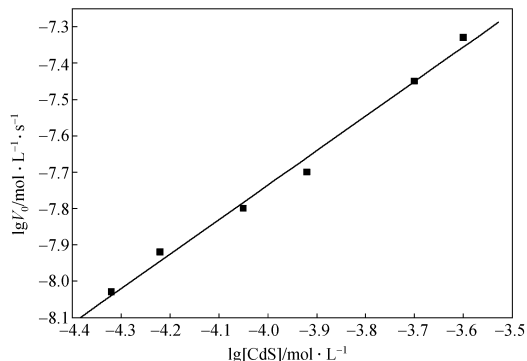


Fig. 6. The initial rate of degradation (V_0) vs. the concentration of $[\text{CdS}]$. Initial concentration of TEMPO is $1.80 \times 10^{-5} \text{ mol/L}$.

When Hys was added, Hys was excited and transferred the electron from the excited state

(Hys^*) to the conduct band of CdS. Then TEMPO was degraded after accepting one electron from conduct band of CdS (reaction (8)). By the initial-rate method (line 2 in fig. 5), $n = 0$. And by the half-life method (line 2 in fig. 7), $n = 0$. Plot 2 (fig. 8(b)) fits curve 1 on the Powell plot, meaning $n = 0$ (for HB). There is the same result in HA-CdS system.

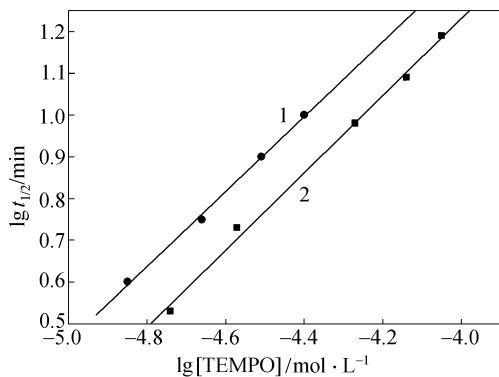


Fig. 7. Dependence of half-life ($t_{1/2}$) on the concentration of TEMPO. 1, $[\text{CdS}] = 1.00 \times 10^{-4} \text{ mol/L}$; 2, $[\text{CdS}] = 6.00 \times 10^{-5} \text{ mol/L}$, $[\text{HB}] = 1.00 \times 10^{-5} \text{ mol/L}$.

In a word, the degradation of spin is a zero-order reaction for TEMPO and first-order reaction for CdS. We assume that Hys-CdS complex is also a first-order reaction. So when Hys is

added, the photo degradation of TEMPO can be expressed as

$$V = -d[\text{TEMPO}]/dt = k_1([\text{CdS}] - [\text{Hys} - \text{CdS}]) + k_2[\text{Hys} - \text{CdS}], \quad (12)$$

where k_1 and k_2 are the rate constants of CdS and Hys-CdS, respectively. Because the reaction order of TEMPO is zero, $[\text{TEMPO}]$ is omitted. At relatively high CdS concentration, $[\text{Hys} - \text{CdS}]$ can be equated to $K_{\text{app}}[\text{Hys}][\text{CdS}]$, and eq. (12) can be derived:

$$V = k_1[\text{CdS}] + (k_2 - k_1)K_{\text{app}}[\text{Hys}][\text{CdS}]. \quad (13)$$

When $[\text{CdS}]$ (or $[\text{Hys}]$) was kept unchanged, one would expect a linear dependence of V on the $[\text{Hys}]$ (or $[\text{CdS}]$). Indeed the linearities of V vs. $[\text{HB}]$ of the inset in fig. 9 and V vs. $[\text{CdS}]$ in fig. 10 (line 2) for HB-CdS system confirmed eq. (13). This suggests that the assumption of first order for Hys-CdS complex is correct.

According to the kinetics equation determined, it is suggested that the control factor of the

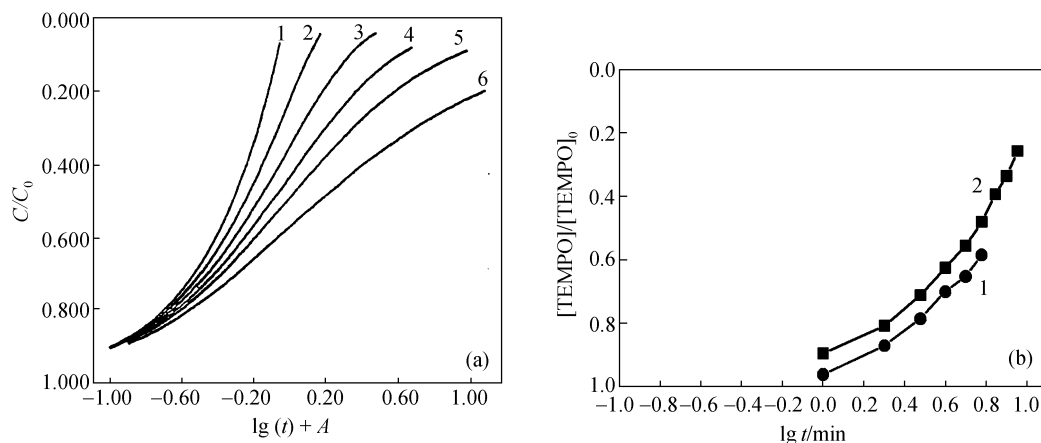


Fig. 8. (a) Powell plot dependence of C/C_0 on $\lg(t)+A$. C/C_0 is how many portions of reaction are left, C_0 is the reactant's initial concentration, $\lg(t)$ is the logarithm of reaction time, A is a constant for each reaction. Curves 1—6 represent the dependence of C/C_0 on $\lg(t)$ of some common orders of reaction: 1, zero order; 2, one-half order; 3, first order; 4, 3/2 order; 5, second order; 6, third order. See the text for details. (b) C/C_0 of TEMPO vs. $\lg(t)$. 1, $[\text{HB}] = 0 \text{ mol/L}$, $[\text{CdS}] = 1.00 \times 10^{-4} \text{ mol/L}$; 2, $[\text{HB}] = 1.00 \times 10^{-5} \text{ mol/L}$, $[\text{CdS}] = 6.00 \times 10^{-5} \text{ mol/L}$.

photo-reduction reaction is how fast CdS or the Hys-CdS complex can offer electrons to TEMPO. Nano-sized semiconductor CdS has the colloidal character, particle can adsorb some TEMPO on its surface because of the large interface between particle and solution. But the adsorption effect of a colloidal particle is not very tight, and because particles move fast in the solution, TEMPO's reduced production can be exchanged by TEMPO quickly. Thus when the concentration of TEMPO changed within a range the reaction rate would not drop, that is, it is zero order for TEMPO in this system. But in the degradation of TEMPO in HA system^[13], there is first-order reaction for TEMPO even if it is in the same range or of higher concentration. That is, when $[\text{TEMPO}]$ was reduced, the reaction rate of HA system would slow down for the limitation of TEMPO. Because of the colloid character, the reactions taking place on the surface of the CdS colloid can be quick and thorough.

When excited with visible light, both singlet and triplet excited states of sensitizers are capable of injecting charge into the semiconductor. But the surface potential, the diffusion length, and the energy difference between excited sensitizer and the conduction band of the semiconductor are expected to influence the kinetics of the charge injection process. There is little driving force for $^3\text{Hys}^*$ ($\mu \geq -0.20 \text{ V}$ (vs. NHE)) as compared to that for $^1\text{Hys}^*$ ($\mu < -0.50 \text{ V}$ (vs. NHE)) to inject an electron into the conduction band of the semiconductor. In addition, the rate of the electron injection process obtained from fluorescence lifetime measurement is $>5.00 \times 10^9 \text{ s}$, but the rate constant k_{isc} of intersystem crossing from S_1 to T_1 is $\sim 10^8 \text{ s}^{-1}$ ^[15], which means that the electron transfer from singlet state of Hys performs much more efficiently than intersystem crossing. So, it is the main way for electron injection from the singlet state of Hys adsorbed on the surface of CdS.

2.4 The kinetics rate constant

Take HB as an example. According to eq. (13), in the absence of HB, there will be linear de-

pendence of V on $[\text{CdS}]$ and the slope is k_1 . This is confirmed by straight line 1 of fig. 10. The k_1 determined by the method is $2.00 \times 10^{-4} \text{ s}^{-1}$. Table 1 shows that the rates of CdS were not changed at different pH scales, that is, the reaction order of $[\text{H}^+]$ in eq. (9) is zero, which means that the electron transferring from CdS to TEMPO is the restrictive process.

Table 1 The photoreduction rate of CdS ($1.80 \times 10^{-4} \text{ mol/L}$) at different pH scales

pH	4.70	7.10	9.20
$V_0 \times 10^8 / \text{mol} \cdot \text{L}^{-1} \cdot \text{s}^{-1}$	3.20	3.10	3.40

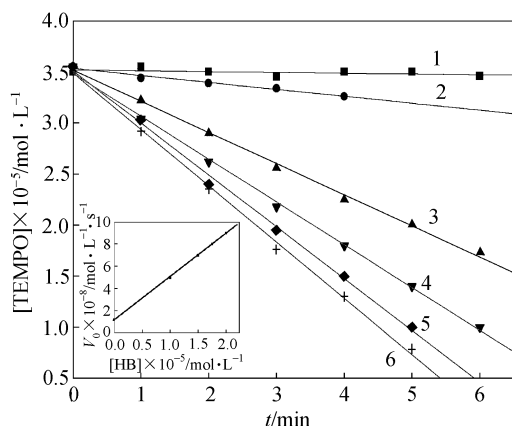


Fig. 9. Concentration of TEMPO vs. irradiation time. $[\text{CdS}]$: 1, 0 mol/L; 2–6, $6.00 \times 10^{-5} \text{ mol/L}$. $[\text{HB}]$: 1, $1.75 \times 10^{-5} \text{ mol/L}$; 2, 0 mol/L; 3, $1.00 \times 10^{-5} \text{ mol/L}$; 4, $1.50 \times 10^{-5} \text{ mol/L}$; 5, $1.75 \times 10^{-5} \text{ mol/L}$; 6, $2.00 \times 10^{-5} \text{ mol/L}$. Inset: the relationship between degradation rate and concentration of HB, when $[\text{CdS}]$ is $6.00 \times 10^{-5} \text{ mol/L}$.

When $[\text{HB}]$ was kept constant, the degradation rate of TEMPO linearly depended on $[\text{CdS}]$ and this straight line's slope was $1.00 \times 10^{-3} \text{ s}^{-1}$ (fig. 10, plot 2). This linearity matched well with eq. (13), and according to this equation the slope was $k_1 + (k_{2(\text{HB}-\text{CdS})} - k_1)K_{\text{app}}[\text{HB}]$. Based on values determined above, the slope was calculated to be $9.30 \times 10^{-4} \text{ s}^{-1}$ which matched well with the value measured. The lines' intercept is zero. This confirms that HB will not reduce TEMPO in this experience condition without CdS. In the same way, for HA-CdS complex system, $k'_1 = 2.18 \times 10^{-4} \text{ s}^{-1}$, $k_{2(\text{HA}-\text{CdS})} = 8.07 \times 10^{-2} \text{ s}^{-1}$. The k'_1 also matched well with the value of $2.00 \times 10^{-4} \text{ s}^{-1}$ determined independently.

When $[\text{CdS}]$ was kept constant, with the addition of HB, the degradation of TEMPO became faster (fig. 9). According to eq. (13), when $[\text{HB}]$ is increased, the degradation rate will linearly depend on $[\text{HB}]$ with the slope equal to $(k_{2(\text{HB}-\text{CdS})} - k_1)K_{\text{app}}[\text{CdS}]$ and the intercept equals $k_1[\text{CdS}]$. The insert of fig. 9 confirmed this linearity. Values of k_1 and $k_{2(\text{HB}-\text{CdS})}$ determined from this plot were $2.10 \times 10^{-4} \text{ s}^{-1}$ and $7.20 \times 10^{-2} \text{ s}^{-1}$, respectively. The k_1 matched well with the value of $2.00 \times 10^{-4} \text{ s}^{-1}$ determined independently. HB cannot cause the degradation of TEMPO alone without CdS in this experience condition ($[\text{HB}] \sim 10^{-6} - 10^{-5} \text{ mol/L}$). Line 1 of fig. 9 confirmed this.

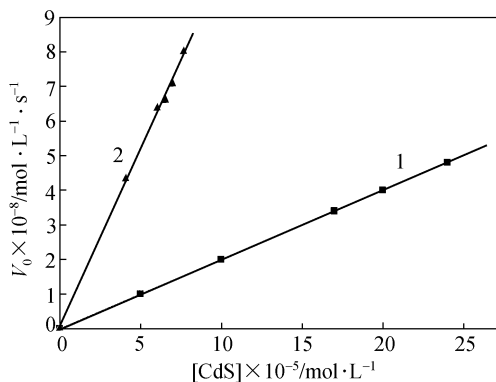


Fig. 10. Dependence of degradation rate on the concentration of CdS. The initial concentration of TEMPO is $2.70 \times 10^{-5} \text{ mol/L}$. 1, Without HB; 2, $[\text{HB}] = 1.00 \times 10^{-5} \text{ mol/L}$.

Because TEMPO's degradation rate depends on how fast CdS or Hys-CdS complex can offer electron, based on k_1 and k_2 determined above, both HA-CdS and HB-CdS complexes are about 350 times more efficient in offering electrons than the CdS semiconductor.

The possible pathway of electron transfer from excited state Hys to CdS is shown in fig. 11. When Hys was excited, it reaches $^1\text{Hys}^*$. If the $^1\text{Hys}^*$ connects CdS particles efficiently, the electron can transfer to the conduction band (CB) of the colloidal semiconductor. Of course, $^1\text{Hys}^*$ can also undergo intersystem crossing to $^3\text{Hys}^*$, the triplet state of Hys

which survives for a longer period of ($\tau_{(T)} \approx 4 \mu\text{s}$)^[16] participates in diffusion-controlled interfacial-transfer process. A small percentage of electrons in the CB came from the VB (valance band) of CdS when CdS was excited. The electrons in CB can reduce TEMPO adsorbed by CdS particles. The irradiation we used was visible light, in this range the absorption of CdS sol. is limited. The concentration of Hys is very low (10^{-6} — 10^{-5} mol/L in the experiment). At such a low concentration, Hys cannot reduce TEMPO directly. But when connected with CdS sol. Hys can improve the photo-reduction efficiency of CdS greatly, which implies that Hys-CdS system is an economic association to make highly efficient photochemical materials.

3 Conclusions

Determined from the fluorescence quenching, the apparent association constants (K_{app}) between Hypocrellin A (HA), Hypocrellin B (HB) and CdS sol. were about $940 (\text{mol/L})^{-1}$, $934 (\text{mol/L})^{-1}$, respectively. Fluorescence lifetime measurements gave the rate constant for the electron transfer process from $^1\text{HA}^*$, $^1\text{HB}^*$ into conduction band of CdS semiconductor as $5.16 \times 10^9 \text{ s}^{-1}$, $5.10 \times 10^9 \text{ s}^{-1}$, respectively. EPR was successfully used to determine the kinetics equation of degradation of TEMPO on the surface of colloidal semiconductors. Using this method the rate constants of reduction reaction taking place on the surface of CdS and Hys-CdS complexes were measured. By comparing rate constants, the Hys-CdS systems were revealed to be about 350 times more efficient than CdS sol. alone in the photoreduction of TEMPO under visible light. It suggests that Hys can be used as an efficient sensitizer of a colloidal semiconductor in the application of solar energy.

Acknowledgements The authors thank Prof. Zhang Xingkang and other colleagues in the laboratory, Institute of Chemistry; and Profs. Hu Jungai and Li Meifeng, Institute of Biophysics, Chinese Academy of Sciences, for their warmhearted help in fluorescence lifetime measurement and EPR experiments. This work was supported by the National Natural Science Foundation of China (Grant No. 39870221).

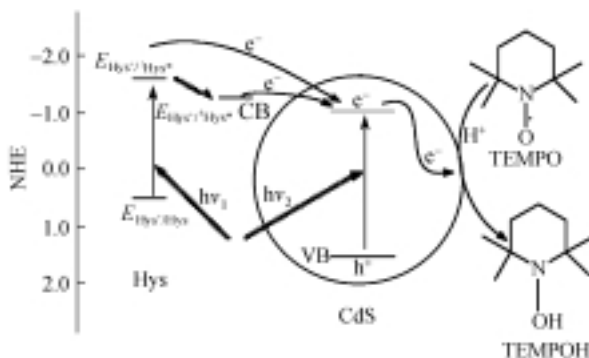


Fig. 11. The possible pathway of photo-induced electron transfer with a schematic diagram describing the CB and VB levels for CdS and electron donating energy levels for Hys. See text for details.

References

1. Henglein, A., Small-particle research: physical-chemical properties of extremely small colloidal metal and semiconductor particles, *Chem. Rev.*, 1989, 89: 1861—1873.
2. Serpone, N., Pelizzetti, E., eds., *Photocatalysis—fundamentals and applications*, New York: Wiley, 1989.
3. Kamat, P. V., Photoelectrochemistry in particulate systems. 9. Photosensitized reduction in a colloidal TiO₂ system using anthracene-9-carboxylic acid as the sensitizer, *J. Phys. Chem.*, 1989, 93: 859—864.
4. Usami, A., Theoretical study of charge transportation in dye-sensitized nanocrystalline TiO₂ electrodes, *Chemical Physics Letters*, 1998, 292: 223—228.
5. Jiang Lijin, Structures, properties, photochemistry reactions and its mechanisms (I)—The structures and properties of hypocrellins, *Chinese Science Bulletin*, 1990, 35(21): 1608—1616.
6. Pivera, J. L., Gracia-jimenez, J. M., Silva Gonzalez, R. et al., Characterization of thin CdS films grown by the gradient recrystallization and growth technique, *J. Appl. Phys.*, 1990, 68(3): 1375—1377.
7. Henglein, A., Mechanism of reactions on colloidal microelectrodes and size quantization effects, *Topics in Current Chemistry*, 1988, 143: 113—180.
8. Kamat, P. V., Chanvet, J. P., Fessenden, R. W., Photoelectrochemistry in particulate systems. 4. Photosensitization of a TiO₂ semiconductor with a chlorophyll analogue, *J. Phys. Chem.*, 1986, 90: 1389—1394.
9. Rossetti, R., Brus, L. E., Time-resolved Raman scattering study of adsorbed, semiosidized Eosin Y formed by excited-stated electron transfer into colloidal TiO₂ particles, *J. Am. Chem. Soc.*, 1984, 106: 4336—4340.
10. Yang, J. J., Feng, L. B., Zhang, Z. J. et al., Study of photoreduction of MV²⁺ taking place on the surface of nanosized CdS particle, *Photographic Science and Photochemistry (in Chinese)*, 1995, 13(3): 227—233.
11. He, H. Z., Jiang, X. F., Wang, D. Y., The photophysical characters of hypocrellin A in the capsule solution, *Photographic Science and Photochemistry (in Chinese)*, 1992, 10(3): 193—199.
12. Diwu Zhenjun, William, L. J., Photosensitization by anticancer agents. 12. Perylene quinonoid pigments, a novel type of singlet oxygen sensitizer, *J. Photochem Photobiol A: Chem.*, 1992, 64: 273—287.
13. Ira N Leveine, *Physics Chemistry*, 2nd ed., New York: McGraw-Hill, 1983.
14. Wang Nenghui, Zhang, Z. Y., Relationship between photosensitizing activities and chemical structure of Hypocrellin A and B, *J. Photochem. Photobiol. B: Biol.*, 1992, 14: 207—217.
15. Zhang, M. H., Weng, M., Chen, S. et al., Study of electron transfer interaction between hypocrellin and N,N-diethylaniline by UV-visible, fluorescence, electron spin resonance spectra and time-resolved transient absorption spectra, *J. Photochem. Photobiol. A: Chem.*, 1996, 96: 57—63.
16. Xia, W. L., Zhang, M. H., Jiang, L. J. et al., Study of hypocrellin A by nanosecond transient absorption spectra, *Science in China (in Chinese)*, Ser. B, 1992, (3): 230—235.